BMC Plant Biology

RESEARCH

Open Access

Plant ubiquitin E2 enzymes UBC32, UBC33, and UBC34 are involved in ERAD and function in host stress tolerance

Chaofeng Wang[1], Bangjun Zhou[1], Yi Zhang[1,2] and Lirong Zeng[1*]

Abstract

Background Endoplasmic reticulum (ER)-associated protein degradation (ERAD) is a critical component of the ER-mediated protein quality control (ERQC) system and plays a vital role in plant stress responses. However, the ubiquitination machinery underlying plant ERAD—particularly the ubiquitin-conjugating enzymes (E2s)—and their contributions to stress tolerance remain poorly understood.

Results In this study, we identified UBC32, UBC33, and UBC34 as ER-localized ubiquitin E2 enzymes involved in ERAD and demonstrated their roles in biotic and abiotic stress tolerance in tomato (*Solanum lycopersicum*) and Arabidopsis (*Arabidopsis thaliana*). In response to biotic stress, UBC33 and UBC34 collectively contribute more substantially than UBC32 to plant immunity against *Pseudomonas syringae* pv. *tomato* (*Pst*). Under abiotic stress and ER stress induced by tunicamycin (TM), all three E2s play important roles. Notably, mutation of UBC32 enhances tolerance to TM-induced ER stress, whereas the loss of function in UBC33 or UBC34 suppresses this response. Additionally, UBC32, UBC33, and UBC34 act synergistically in Arabidopsis seed germination under salt stress and abscisic acid (ABA) treatment. While the single mutants *atubc32*, *atubc33*, and *atubc34* exhibit germination rates comparable to Col-0 under salt stress or ABA treatment, the double mutants *atubc32/33*, *atubc32/34*, and *atubc33/34* show a significantly greater reduction in germination rate. Interestingly, the *atubc32/33/34* triple mutant exhibits a seed germination rate under salt stress and ABA treatment, as well as a level of host immunity to *Pst*, comparable to that of the *atubc33/34* and *atubc32/34* double mutants.

Conclusions Our findings establish UBC32, UBC33, and UBC34 as key components of the plant ERAD machinery, contributing to plant tolerance to both abiotic and biotic stress. Despite their close phylogenetic relationship, these E2 enzymes exhibit redundant, synergistic, or antagonistic roles depending on the specific stress response pathway, underscoring the complexity of their functional interactions.

Keywords Endoplasmic reticulum (ER)-associated protein degradation (ERAD), ER stress, Abiotic stress, Biotic stress, Ubiquitin-conjugating enzyme (E2), *Pseudomonas syringae* Pv. *tomato*

*Correspondence:
Lirong Zeng
lzeng3@unl.edu
[1]Center for Plant Science Innovation and Department of Plant Pathology, University of Nebraska, Lincoln, NE 68588, USA
[2]Present address: South China Botanical Garden, Chinese Academy of Sciences, Guangzhou 510650, China

Background

Plants, due to their sessile nature, continuously face abiotic and biotic stresses throughout their lifecycle. To adapt to these challenges,, plants have evolved sophisticated stress response mechanisms [1, 2]. Among these, ubiquitination—a major posttranslational modification in eukaryotic cells—has emerged as a key regulatory process governing plant responses to various environmental stresses, including extreme temperatures (heat and cold), low oxygen availability, drought, salt, nutrient deficiency, and pathogen infections [3–5]. More than 130 ubiquitin ligases have been implicated in plant responses to different abiotic stresses [6], with several targeting key components of the abscisic acid (ABA) signaling pathway, which is central to drought- and salt-stress responses [5, 7]. In recent years, increasing attention has also been directed toward the role of ubiquitination in plant immunity, with modifications of key immune signaling components by different ubiquitin chains having been reported [3, 8, 9].

Protein ubiquitination is a hierarchical, multi-step process catalyzed by three classes of enzymes: ubiquitin-activating enzyme (E1 or UBA), ubiquitin-conjugating enzyme (E2 or UBC), and ubiquitin ligase (E3). Through this E1-E2-E3 enzymatic cascade, one or more ubiquitin molecules are covalently attached to substrate proteins. First, the E1 enzyme activates ubiquitin in an ATP-dependent manner, leading to the formation of a thioester linkage between the ubiquitin C-terminus and the catalytic cysteine of E1. The activated ubiquitin is then transferred to an E2 enzyme via transesterification. Finally, an E3 ligase facilitates ubiquitin transfer from the E2 enzyme to specific substrate proteins, determining substrate specificity in the ubiquitination process.

A plant genome typically encodes several E1s, dozens of E2s, and hundreds of E3s [10]. This organization of the enzymatic cascade can be visualized as a pyramid, with E1 enzymes at the apex initiating ubiquitination, while E3 ligases at the base provide substrate specificity. Due to their apparent importance in ubiquitination, E1 and E3 enzymes have been the focus of many studies in this field. In contrast, E2 enzymes were historically considered to play only an auxiliary role in ubiquitin transfer and thus received less attention. However, this perspective has gradually shifted with discoveries showing that E2 enzymes play a critical role in determining the length and topology of the polyubiquitin chains and the processivity of the chain formation in ubiquitination [11].

Endoplasmic reticulum (ER)-associated protein degradation (ERAD) is an essential component of ER-mediated protein quality control (ERQC) system. ERQC ensures proper folding of nascent membrane and secretory proteins while selectively degrading terminally misfolded proteins via ERAD [12, 13]. In this pathway, terminally misfolded proteins in the ER are first recognized by adaptor proteins, such as HRD3, and recruited to ER membrane-anchored E3 ligase complexes, including the HRD1 (HMG-COA Reductase Degradation 1) and the DOA10 (Degradation Of Alpha2 10) complexes. These proteins are then retro-translocated, ubiquitinated, and degraded by the 26 S proteasome in the cytoplasm [13, 14]. ERAD plays a crucial role in various physiological processes. In humans and animals, ERAD dysfunction is associated with over 60 diseases, including neurodegenerative disorders, diabetes, atherosclerosis, and cancer [15, 16]. In plants, ERAD has emerged as a key regulator of responses to both biotic and abiotic stresses [17]. Consequently, identifying and characterizing the ubiquitination machinery responsible for ERAD is of fundamental importance.

In yeast and animals, multiple ERAD components have been identified, including E3 ligases, such as HRD1, gp78 (Glycoprotein 78), RMA1 (RING Membrane Anchor1), Parkin, CHIP (C-terminus of Hsc70-interacting protein), and DOA10, as well as E2 enzymes such as UBC6 and its homologs UBE2J1 and UBE2J2, and UBE2G2/UBC7 [15, 18–20]. In plants, homologs of several ERAD-associated E3 ligases, including HRD1, RMA1, DOA10, have been identified. Additionally, plant-specific ERAD-associated E3 ligases, such as MfSTMIR (*MEDICAGO falcata* Salt Tunicamycin-Induced Ring Finger Protein), EMR (ERAD-mediating RING finger protein), and DGS1 (Decreased Grain Size1) have been reported [17, 21]. However, only a limited number of plant E2 enzymes have been explicitly linked to ERAD. The Arabidopsis E2 enzyme AtUBC32 and its rice ortholog OsUBC45 are the only plant E2s demonstrated to function in ERAD and contribute to stress tolerance, including stress induced by reactive oxygen species, salt, and drought [22, 23]. Notably, OsUBC45 overexpression enhances resistance to rice blast and bacterial leaf blight diseases [24]. More recently, rice SMG3 (Small Grain 3, also known as OsUBC45) was found to interact with DGS1 (Decreased Grain Size1) to regulate grain size and weight through the brassinosteroid (BR) signaling pathway [21]. Phylogenetic analyses have placed the E2 enzymes UBC32, UBC33, and UBC34 to the same subgroup in Arabidopsis (group XIV) and in tomato (group IV) [25, 26]. While UBC32 has been established as a component of the ERAD pathway in Arabidopsis [27], direct evidence supporting the involvement of UBC33 and UBC34 in ERAD remains lacking, despite their confirmed ER localization in Arabidopsis [28]. Compared to UBC32, functional studies of UBC33 and UBC34 remain limited, and apart from OsUBC45, no ERAD-associated E2 enzymes have been reported to function in plant immunity.

Our previous study identified 40 ubiquitin E2 proteins in tomato (*Solanum lycopersicum*) and classified them into 13 phylogenetic groups [26]. Among these, members

of the group III were found to be redundantly essential for plant innate immunity and are exploited by AvrPtoB, a *Pseudomonas syringae* pv *tomato* (*Pst*) type III effector encoding an ubiquitin E3 ligase, to suppress the tomato receptor-like kinase Fen-mediated host immunity [26]. To further understand the roles of plant ubiquitin E2 enzymes, particularly those involved in plant ERAD, we systematically investigated UBC32, UBC33, and UBC34 in tomato and Arabidopsis in this study. Our findings reveal that, like UBC32, UBC33 and UBC34 also function in ERAD and contribute to plant abiotic and biotic stress tolerance. Notably, while all three E2 enzymes participate in plant abiotic and biotic stress responses, they exhibit redundant, synergistic, or antagonistic roles in these pathways, depending on the context.

Results

Tomato group IV E2s are ER-Localized

Our previous study demonstrated that the tomato (*Solanum lycopersicum*) group IV E2s—SlUBC32, SlUBC33, and SlUBC34—share a close phylogenetic relationship with their Arabidopsis counterparts, based on a genome-wide identification and characterization of tomato ubiquitin E2 enzymes [26]. Sequence alignment with Arabidopsis AtUBC32, AtUBC33, and AtUBC34, as well as mammalian UBE2J1 and UBE2J2, which are known to be involved in ERAD, reveals high homology of SlUBC32, SlUBC33, and SlUBC34 with these E2 enzymes (Supplementary Fig. 1). These results suggest that the three tomato E2 enzymes might also participate in ERAD. To test this hypothesis, we first examined their subcellular localization by co-expressing the SlUBC32, SlUBC33, or SlUBC34 fused with green fluorescent protein (GFP) and the ER marker ER-rb fused with mCherry [29] in tobacco leaves through *Agrobacterium*-mediated transient expression. As shown in Fig. 1, the SlUBC32-GFP, SlUBC33-GFP, and SlUBC34-GFP localized to reticular structures that perfectly overlapped with the ER networks formed by the ER-rb proteins. These

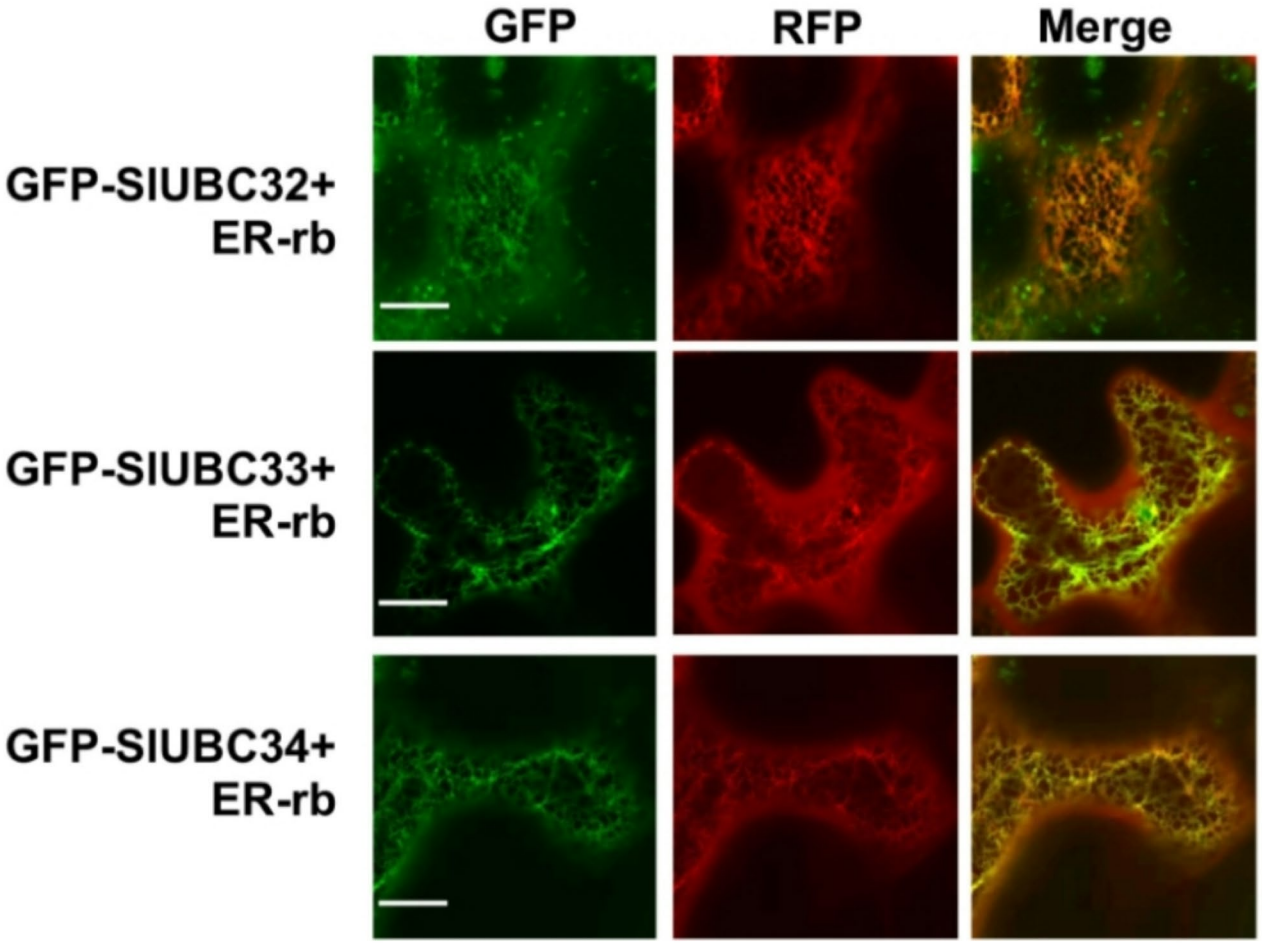

Fig. 1 Subcellular localization of tomato E2 enzymes SlUBC32, SlUBC33 and SlUBC34. GFP-fused SlUBC32, SlUBC33 and SlUBC34 were co-expressed with ER-localized marker protein-fused with mCherry (ER-rb) into tobacco leaves. Fluorescence signals were observed by confocal microscopy 48 h after Agro-infiltration. The expressed proteins were observed by confocal microscopy 48 h after infiltration. Bars = 20 μm

results indicate that the tomato group IV E2s, SlUBC32, SlUBC33, and SlUBC34 are ER-localized.

Tomato group IV E2s interact with ERAD-Related E3 ubiquitin ligase

Next, we examined whether SlUBC32, SlUBC33, and SlUBC34 interact with known ERAD-associated E3 ubiquitin ligases. Among the E3s implicated in ERAD, HRD1 and its homologs are present across yeast, mammals and plants. We identified the tomato SlHRD1 by searching the tomato genome with the two Arabidopsis HRD1 genes, *AtHRD1A* and *AtHRD1B*, as queries. Two tomato homologous genes, *SlHRD1A* (Solyc03g096930.2.1) and *SlHRD1B* (Solyc06g072790.2) were identified (Supplementary Data File I). Protein sequence alignment of Arabidopsis, tomato and the yeast (*Saccharomyces cerevisiae*) HRD1 homologs indicated that the HRD1 homologs from the two plant species share relatively higher homology (65.98 – 76.32% of amino acid identity), whereas the homology between yeast and plant HRD1 proteins is low (22.39 – 23.09% of amino acid identity) (Supplementary Figs. 2A and 2B), as supported by phylogenetic analysis (Supplementary Fig. 2C). Both Arabidopsis and tomato HRD1 homologs are predicted to possess six transmembrane helices within the N-terminal half of the protein and a RING domain approximately in the central region of the protein (Supplementary Fig. 2A). The sequences of the N-terminal half and the RING domain of the Arabidopsis and tomato HRD1 homologs are highly conserved, whereas the sequences near the C-terminal region show high variation.

Subcellular localization assays showed that the SlHRD1A and SlHRD1B proteins are ER-bound (Fig. 2A). In these assays, the fluorescence signal from yellow fluorescence protein (YFP)-fused SlHRD1A or SlHRD1B (pseudo-colored in red) overlapped well with the cyan fluorescent protein (CFP) signal (pseudo-colored in green) of CFP-fused ER marker ER-cb [29] in reticulum structures when they were co-expressed in protoplasts derived from tomato leaves, indicating that SlHRD1A and SlHRD1B are indeed ER-resident. Consistent with a previous report [29], localization of the ER marker ER-cb in the tomato protoplasts is specific and significantly distinct from that of the Golgi body marker (Supplementary Fig. 3A). We then systematically tested the interaction of SlUBC32, SlUBC33 and SlUBC34 with the tomato HRD1 homologs using yeast two-hybrid (Y2H) and bimolecular fluorescence complementation (BiFC) assays. In Arabidopsis, the AtHRD3A protein (At1g18260) is the only functional Arabidopsis homolog of the yeast HRD3 adaptor protein for its ERAD-related E3 ligase HRD1 (ScHARD1) [30]. We thus also cloned and included SlHRD3A (Solyc03g118670.3.1), the tomato homolog of AtHRD3A in the Y2H assay. As shown in Fig. 2B, SlUBC32, SlUBC33 and SlUBC34 all interact strongly with SlHRD1A, SlHRD1B and the adapter protein SlHRD3A in the Y2H assay using the mating-based split-ubiquitin system (mbSUS), designed for identifying potential interactions between membrane proteins or between a membrane protein and a soluble protein [31]. SlHRD3A showed strong self-interaction in the assay, but its interactions with SlHRD1A, SlHRD1B were weak (Fig. 2B) and thus were not included in the subsequent BiFC assay. The interactions of SlUBC32, SlUBC33 and SlUBC34 with the SlHRD1A and SlHRD1B were further confirmed by the BiFC assay performed using tomato protoplasts. These interactions generated green fluorescence signals, whereas no signals were detected in control (Fig. 2C). To confirm the interactions of SlUBC32, SlUBC33 and SlUBC34 with SlHRD1A and SlHRD1B occur at ER, we randomly tested these interactions by performing the BiFC assay on tobacco (*Nicotiana benthamiana*) leaves and using confocal microscopy. The results indicated that the interactions occur at reticulum structures inside the cell, suggesting they take place at ER (Supplementary Fig. 3B).

Tomato group IV E2s and arabidopsis AtUBC33 and AtUBC34 are active ERAD components

The interaction of SlUBC32, SlUBC33 and SlUBC34 with tomato HRD1 proteins suggests that they likely play active roles in ERAD. To test this hypothesis, we assessed the stability of MLO-12, a known plant ERAD substrate protein, under conditions where these group IV E2 genes were either overexpressed or knocked down [27, 32]. Compared to the control, transient co-expression of MLO-12 with individual members of the group IV E2s promoted MLO-12 degradation (Fig. 3A, left panel). Consistent with the previous report that MLO-12 is a proteasome-dependent ERAD substrate [32], treatment with 75 μM MG132 for 30 min inhibited the promoted degradation of MLO-12 when co-expressed with members of the group IV E2s (Fig. 3A, right panel). In contrast, knocking down *UBC32* and *UBC33/34* by virus-induced gene silencing (VIGS) enhanced MLO-12 accumulation (Fig. 3B), suggesting that SlUBC32, SlUBC33 and SlUBC34 are involved in ERAD. *Nicotiana benthamiana*, a solanaceae species closely related to tomato, has been used as a model plant for studying molecular plant-bacteria interactions. The *N. benthamiana* genome encodes a full set of the tomato E2 counterparts [26]. Consistently, MLO-12 degradation was reduced in the *N. benthamiana* RNAi transgenic lines *NbUBC32i* and *NbUBC33/34i* (Fig. 3C). Together, these results confirm that SlUBC32, SlUBC33 and SlUBC34 are active components of the ERAD apparatus.

Although AtUBC32 has been explicitly demonstrated to be a functional ERAD component, no reports have

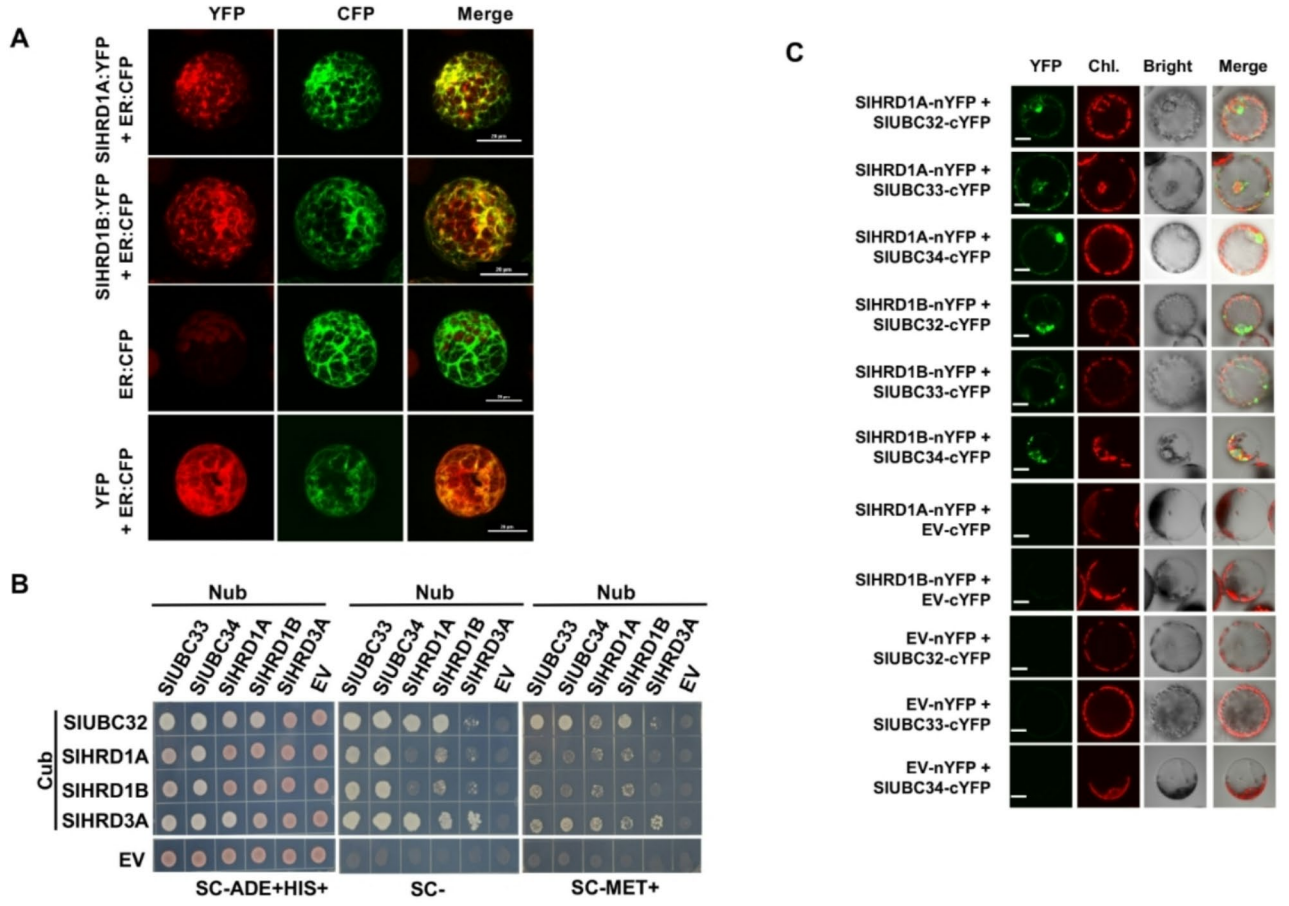

Fig. 2 SlUBC32, SlUBC33 and SlUBC34 interact with ER-bound E3 ubiquitin ligases SlHRD1A and SlHRD1B. (**A**) Subcellular localization of tomato homologs of the ERAD E3s, SlHRD1A and SlHRAD1B. An ER localized marker that was fused with CFP (pseudo-colored in green) and SlHRD1A and SlHRD1B that was fused with YFP (pseudo-colored in red) were transiently co-transfected in Arabidopsis mesophyll protoplasts. Z-stack fluorescence images of single cell were observed with a confocal microscope. Bars = 20 μm. (**B**) SlUBC32, SlUBC33 and SlUBC34 interact with SlHRD1A and SlHRD1B, the tomato homolog of HRD1, and their adapter protein SlHRD3A in the mating-based split ubiquitin yeast two-hybrid system. Growth of yeast cells harboring two genes that had been fused with the N-terminal (Nub) and C-terminal (Cub) halves of the ubiquitin protein, respectively on SC-ADE$^+$HIS$^+$, SC- and SC- plus 0.15 M MET media plates, respectively, were shown in the left, middle and right panel, respectively. Empty bait and prey vector (EV) were used as control. (**C**) SlUBC32, SlUBC33 and SlUBC34 interact with SlHRD1A and SlHRD1B in BiFC assay using tomato leaf protoplasts. YFP signal (pseudo-colored in green) indicates the interaction of corresponding co-expressed proteins. EV, empty vector; Chl., chlorophyll autofluorescence colored in red; Bright, bright field image. Bars = 20 μm

addressed the involvement of AtUBC33 and AtUBC34 in ERAD to date. Based on our findings for SlUBC32, SlUBC33 and SlUBC34, we inferred that AtUBC33 and AtUBC34 are also functionally active ERAD components. To confirm this, we obtained Arabidopsis T-DNA insertion mutant lines of *AtUBC32*, *AtUBC33*, and *AtUBC34* (Supplementary Fig. 4A) and generated homozygous double and triple mutant lines (*atubc32/33*, *atubc32/34*, *atubc33/34*, and *atubc32/33/34*) by crossing. These mutants were confirmed by genotyping PCR (Supplementary Fig. 4B). The transcripts of the *AtUBC32*, *AtUBC33* and *AtUBC34* genes were examined to confirm the knockout efficiency in the corresponding mutants using semi-quantitative RT-PCR (Supplementary Fig. 4C). No significant morphological changes are observed between Col-0 and the mutants. The *atubc33*, *atubc34*, *atubc32/33*, *atubc33/34* and *atubc32/33/34* mutant plants are slightly smaller than Col-0, whereas the *atubc32/34* mutant line is noticeably smaller than Col-0 (Supplementary Figs. 5 and 6). The *atubc32*, *atubc33*, *atubc34* single, double, and triple mutant lines display slightly earlier flowering than Col-0 (Supplementary Fig. 6).

As we examined of SlUBC32, SlUBC33 and SlUBC34 for their roles in ERAD (Fig. 3A and C), we tested the stability of MLO-12 in protoplasts derived from Col-0 and the single, double and triple mutants of *AtUBC32*, *AtUBC33*, and *AtUBC34*. Consistent with a previous report [27], the null mutation in *AtUBC32* diminished the MLO-12 degradation (Fig. 3D). Similarly, loss of function in AtUBC33 and AtUBC34 also reduced the MLO-12 turnover, indicating their involvement in ERAD.

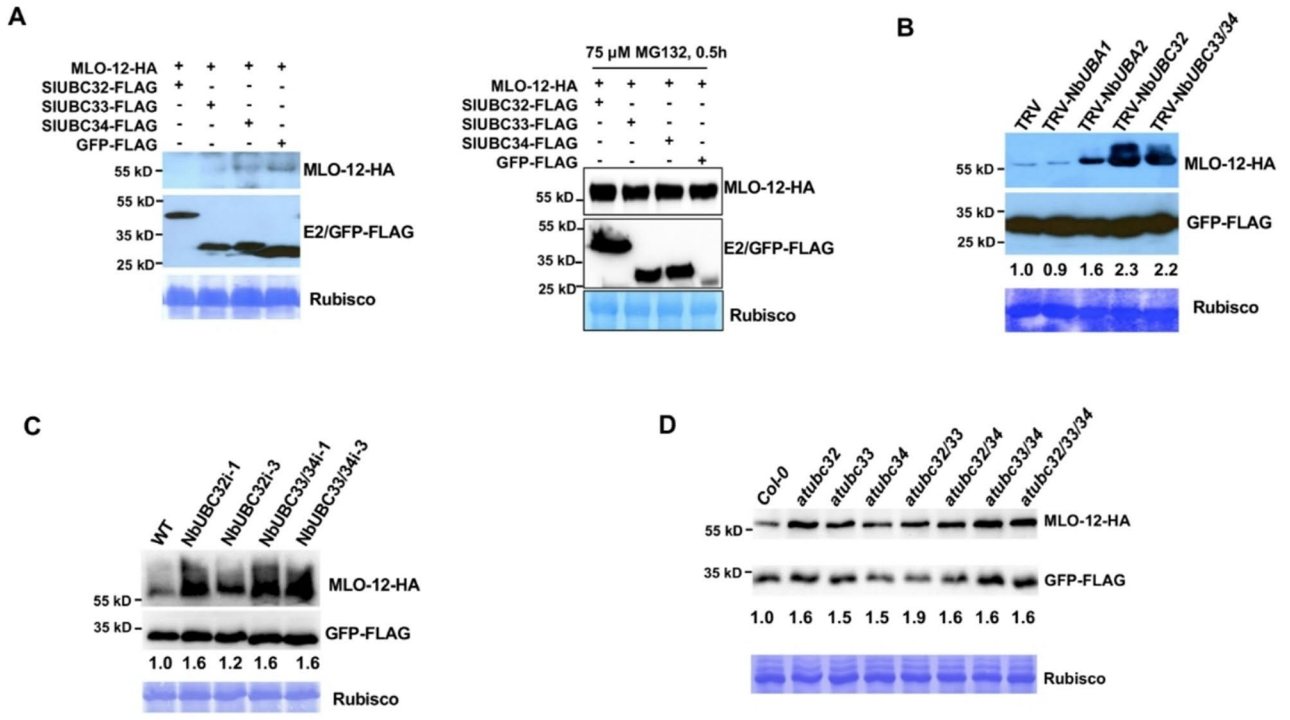

Fig. 3 Tomato, *N. benthamian* and *Arabidopsis* UBC32, UBC33, and UBC34 are involved in ERAD. (**A**) Transient co-expression of SlUBC32, SlUBC33 and SlUBC34 and the well-known ERAD target protein MLO-12 increased degradation of MLO-12 in tobacco leaves (left panel) and treatment with 75 μM MG132 for 30 min inhibited this increased degradation (right panel). GFP was used as control. (**B**) Knocking down *NbUBC32*, *NbUBC33* and *NbUBC34* in leaves of *N. benthamian* plants by VIGS reduced the degradation of MLO-12. The E1 enzymes NbUBA1 and NbUBA2, which were found to play distinct roles in plant immunity by our unpublished data, were used as control. (**C**) Degradation of MLO-12 was reduced in *N. benthamian* RNAi transgenic lines where *NbUBC32*, *NbUBC33* and *NbUBC34* genes were silenced. Two independent transgenic lines in which the *NbUBC32* gene and the *NbUBC33* and *NbUBC34* genes were silenced, respectively were used for the assay. (**D**) Degradation of MLO-12 was reduced in *Arabidopsis* T-DNA insertion mutants of the *AtUBC32*, *AtUBC33*, and *AtUBC34* genes. In (**B**), (**C**), and (**D**), the numbers below the GFP band denote the relative abundance of the MLO-12 proteins by quantifying the pixel density of the MLO-12-HA band and normalizing to the pixel density of the corresponding GFP-FLAG band using the ImageJ software, with the relative abundance of the corresponding control sample set as 1.0. The FLAG-tagged GFP was expressed together with HA-tagged MLO-12 as an internal control of efficiency in transient gene expression as well as control of non-misfolded protein. Staining of the Rubisco large subunit (Rubisco) by Coomassie Blue R250 denotes equal sample loading

We repeatedly observed less MLO-12 degradation in the *atubc32/33* double mutant than in the *atubc32* and *atubc33* single mutants, suggesting an additive effect of AtUBC32 and AtUBC33 proteins in ERAD. However, we did not observe similar effects in the double mutants containing the *atubc34* mutation (i.e. the *atubc32/34* and *atubc33/34* mutants) (Fig. 3D), suggesting somewhat functional redundancy of AtUBC34 with AtUBC32 and AtUBC33. Additionally, the *atubc32/33/34* triple mutant displayed MLO-12 accumulation comparable to the *atubc32/34 and atubc33/34* double mutants but less than that in the *atubc32/33* double mutant. Together, all the three Arabidopsis E2s—AtUBC32, AtUBC33, and AtUBC34—are active ERAD components.

UBC32, UBC33 and UBC34 are involved in host immunity in tomato and arabidopsis

Quantitative real-time PCR (qRT-PCR) indicated that the expression of *SlUBC32*, *SlUBC33* and *SlUBC34* were significantly induced 2 h after flg22 treatment (Fig. 4A) or 24 h after inoculation with *Pst* DC3000 (Fig. 4B). The expression of *SlUBC33* and *SlUBC34* was also induced at 24 h after inoculation of *Pst* DC3000*ΔhrcQ-U* (Fig. 4B). The growth of the *Pst* DC3000*ΔhrcQ-U* was significantly higher on the tomato plants where the *SlUBC32*, *SlUBC33* and *SlUBC34* genes were efficiently knocked down by VIGS (Supplementary Fig. 7A) compared to the control (TRV) plants on day 3 after inoculation, regardless the method of inoculation (Fig. 4C and D). This suggests that SlUBC32, SlUBC33 and SlUBC34 play key roles in tomato immunity against bacterial pathogens.

To confirm the roles of group IV E2s in plant immunity, we investigated the *NbUBC32*, *NbUBC33*, and *NbUBC34* in *N. benthamiana*. Since *NbUBC33* and *NbUBC34* are highly homologous but have relatively lower homology to *NbUBC32* [26], we developed separate transgenic *N. benthamiana* lines (*NbUBC32i* and *NbUBC33/34i*), where the expression of *NbUBC32* or *NbUBC33/NbUBC34* genes are significantly knocked down (Supplementary Fig. 7B). The growth of the *Pst* DC3000Δ*hopQ1-1* on the

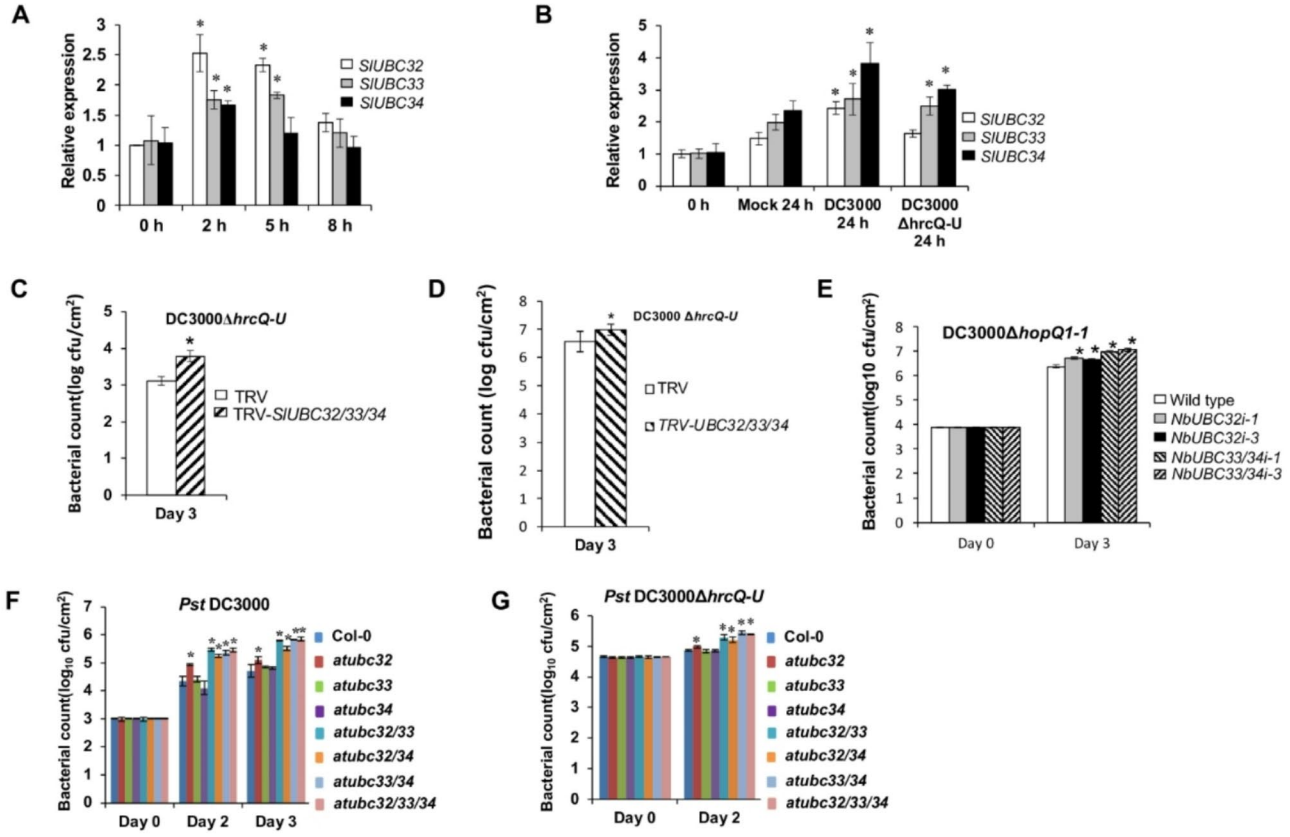

Fig. 4 UBC32, UBC33, and UBC34 are involved in plant immunity. (**A**) and (**B**) The expressions of tomato *SlUBC32*, *SlUBC33* and *SlUBC34* genes were induced by flg22 (**A**) and different *Pst* DC3000 strains (**B**). The expressions of *SlUBC32*, *SlUBC33* and *SlUBC34* were analyzed by qRT-PCR using tomato *EF1a* gene as the internal reference. Error bars indicate standard deviation. Asterisks indicate significantly elevated expression compared to the expression level of corresponding gene at 0 h based on the one-way ANOVA ($P < 0.01$). (**C**) and (**D**) Knocking down the expression of tomato *UBC32*, *UBC33*, and *UBC34* genes significantly increased bacterial growth compared to the control plants infected with the TRV empty vector (TRV) when the vacuum infiltration (**C**) and dipping (**D**) methods were used, respectively to inoculate tomato plants with *Pst* DC3000*ΔhrcQ-U*. (**E**) Knocking down the expression of *N. benthamiana NbUBC32* or *NbUBC33* and *NbUBC34* genes in transgenic plants significantly increased the growth of the bacterial pathogen strain *Pst* DC3000*ΔhopQ1-1* compared to the control plants. (**F**) and (**G**) Bacterial growth assay on Arabidopsis single, double and triple mutants of the *AtUBC32*, *AtUBC33* and *AtUBC34*genes. Wild-type Col-0 and different mutant lines for the *AtUBC32*, *AtUBC33* and *AtUBC34* gene were infected with *Pst* DC3000 strain (**F**) and *Pst* DC3000ΔhrcQ-U strain (**G**). The bacterial population was examined on the indicated days after inoculation. Error bars show standard deviation. For (**C**) - (**G**), asterisks indicate significantly elevated bacterial growth compared with the Col-0 plants based on one-way ANOVA ($P < 0.01$). cfu, colony-forming units

NbUBC32i and *NbUBC33/34i* plants was higher than that on the wild-type *N. benthamiana* plants on day 3 after inoculation (Fig. 4E). Consistently, VIGS-induced silencing of *UBC32*, *UBC33* and *UBC34* in *N. benthamiana* plants also resulted in reduced host immunity (Supplementary Fig. 7C). These findings indicate that, like SlUBC32, SlUBC33 and SlUBC34 in tomato, NbUBC32, NbUBC33, and NbUBC34 play key roles in *N. benthamiana* immunity against bacterial pathogens, suggesting functional conservation for UBC32, UBC33 and UBC34 in host immunity across different plant species.

We further examined the immune roles of UBC32, UBC33, and UBC34 in Arabidopsis. Like the pathogen growth assays we did in tomato and *N. benthamiana* (Fig. 4C and E), we examined pathogen growth on the mutant lines *atubc32*, *atubc33*, *atubc34*, *atubc32/33*, *atubc32/34*, *atubc33/34* and *atubc32/33/34*. Compared with the Col-0, *atubc32*, *atubc32/33*, *atubc32/34*, *atubc33/34* and *atubc32/33/34* were more susceptible to *Pst* DC3000 and DC3000ΔhrcQ-U, as evidenced by significantly increased growth of the pathogens on these lines (Fig. 4F and G). The single mutants *atubc33* and *atubc34* displayed bacterial growth comparable to Col-0, whereas the double mutant *atubc33/34* exhibited significantly increased bacterial growth compared to Col-0, indicating a synergistic effect between *AtUBC33* and *AtUBC34* in host immunity, unlike their functional redundancy in ERAD (Fig. 3D). Similarly, a synergistic effect between AtUBC32 and AtUBC33 in host immunity was observed. While the double mutants *atubc32/33*, *atubc32/34*, and *atubc33/34* were more susceptible to pathogen infection than the single mutant *atubc32*,

atubc33, and *atubc34*, the triple mutant *atubc32/33/34* consistently showed enhanced pathogen growth comparable to the *atubc32/33* double mutant. This observation suggests that, like the effects on ERAD by the *atubc32/33/34* triple mutations (Fig. 3D), a feedback loop likely exists in the cell where the synergistic effects of *atubc32/atubc33*, *atubc33/atubc34*, and *atubc32/atubc34* on host immunity are partially compensated by another ER-associated E2 (or E2s) when AtUBC32, AtUBC33, and AtUBC34 are all mutated. Combining these findings with our discoveries in tomato and *N. benthamiana*, we conclude that the UBC32, UBC33, and UBC34 E2s play key roles in plant immunity against bacterial pathogens, and their roles in host immunity are likely conserved across different plant species.

UBC33 and UBC34 play antagonistic roles to UBC32 in plant ER stress response

The increase of protein synthesis and secretion after pathogen infection can exceed the capacity of protein-folding and degradation at ER, resulting in ER stress response centered on unfolded protein response (UPR) [33, 34]. Both flg22 treatment and pathogen infection induce ER stress response, as evidenced by IRE1 (inositol-requiring enzyme 1)-mediated splicing of the ER stress response gene bZIP60 (Fig. 5A and B) [35]. ER stress responses have been shown to be involved in plant immunity [35, 36]. The diminished host immunity in various *atubc32*, *atubc33* and *atubc34* double and triple mutant lines is likely associated with an impaired plant ER stress response. Consistent with the notion that damage to ERAD would lead to increased misfolded and unfolded proteins, the expression of the UPR marker gene *Bip3* in the mutants was enhanced compared to Col-0 upon treatment with the ER stress agent, tunicamycin (TM) (Supplementary Fig. 8A).

A seedling growth assay indicated that, consistent with a previous report [27], the *atubc32* mutant displayed higher ER-stress tolerance than Col-0 (Fig. 5C and D). However, the *atubc33* and *atubc34* mutants both displayed significantly reduced tolerance to TM-induced ER stress. The *atubc32/33*, *atubc32/34* and *atubc32/33/34* displayed reduced ER-stress tolerance compared to Col-0, suggesting that knocking out of *AtUBC33* and/

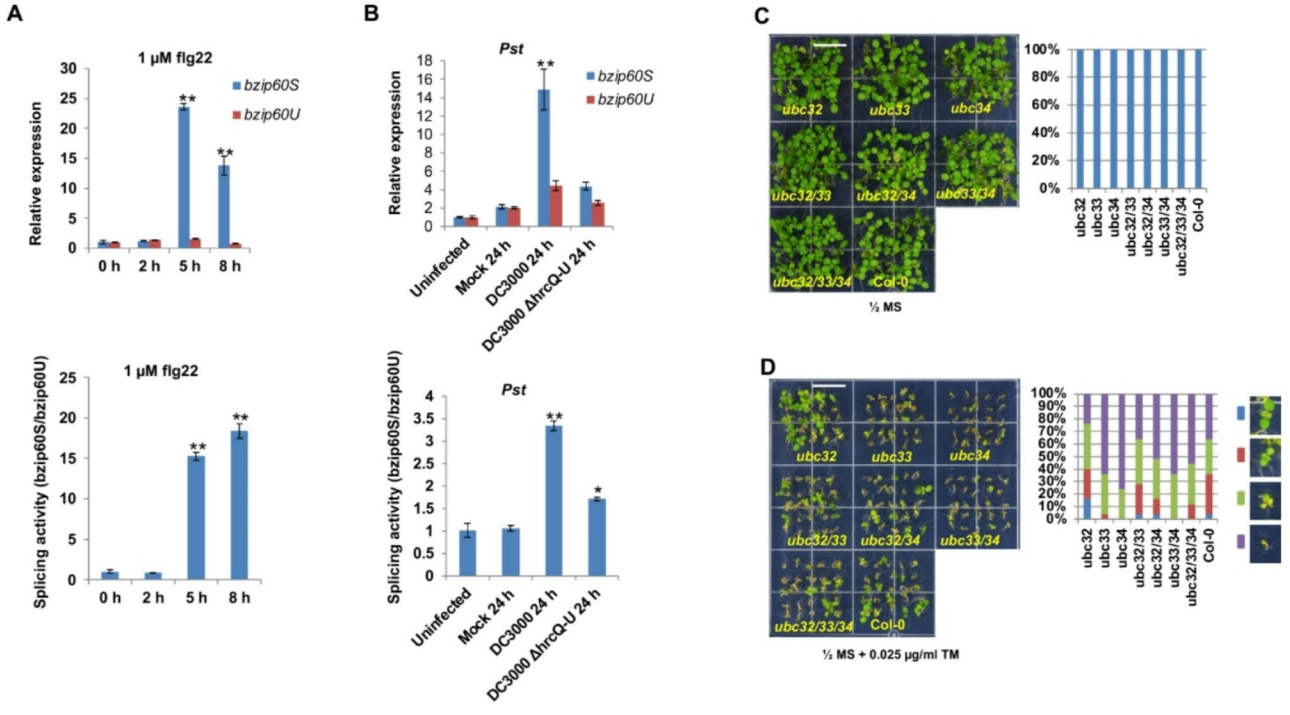

Fig. 5 UBC32, UBC33, and UBC34 play different roles in plant ER stress tolerance. (**A**) and (**B**) ER stress response is involved in plant immunity. Quantitative measurement of bZIP60 mRNA splicing activity was performed by qRT-PCR analyses of spliced (*bzip60S*) and non-spliced (*bzip60U*) *bZIP60* forms. Ratios of *bzip60S* to *bzip60U* are calculated, with the ratio of uninfected Col-0 set as 1. (**A**) qRT-PCR analyses of *bzip60S* and *bzip60U* in 10-day tomato seedlings treated with 1 μM flg22 in half-strength liquid MS media (upper panel). Ratios of spliced *bzip60S* and unspliced *bzip60U* are shown in the low panel. (**B**) Upper panel: qRT-PCR analyses of *bzip60S* and *bzip60U* in 3-week tomato plants infected with *Pst* pathogens by the dipping method. Ratios of spliced *bzip60S* and unspliced *bzip60U* are shown in the low panel. Statistical analysis was performed using Student's t-test. *, $p \le 0.05$. **, $p \le 0.01$. (**C**) and (**D**) The phenotypes of different Arabidopsis *ubc32*, *ubc33* and *ubc34* mutant lines grew on media without (**C**) or with 0.025 μg/mL tunicamycin (**D**) in seedling growth assay. The percentages of different phenotypes are shown in the right panels. A representative image of two independent experiments is shown. For quantification of seedling phenotypes, $n \ge 30$ (right panel). White bar = 1.0 cm. Photos were taken 7 days after sowing cold-stratified seeds on the growth media

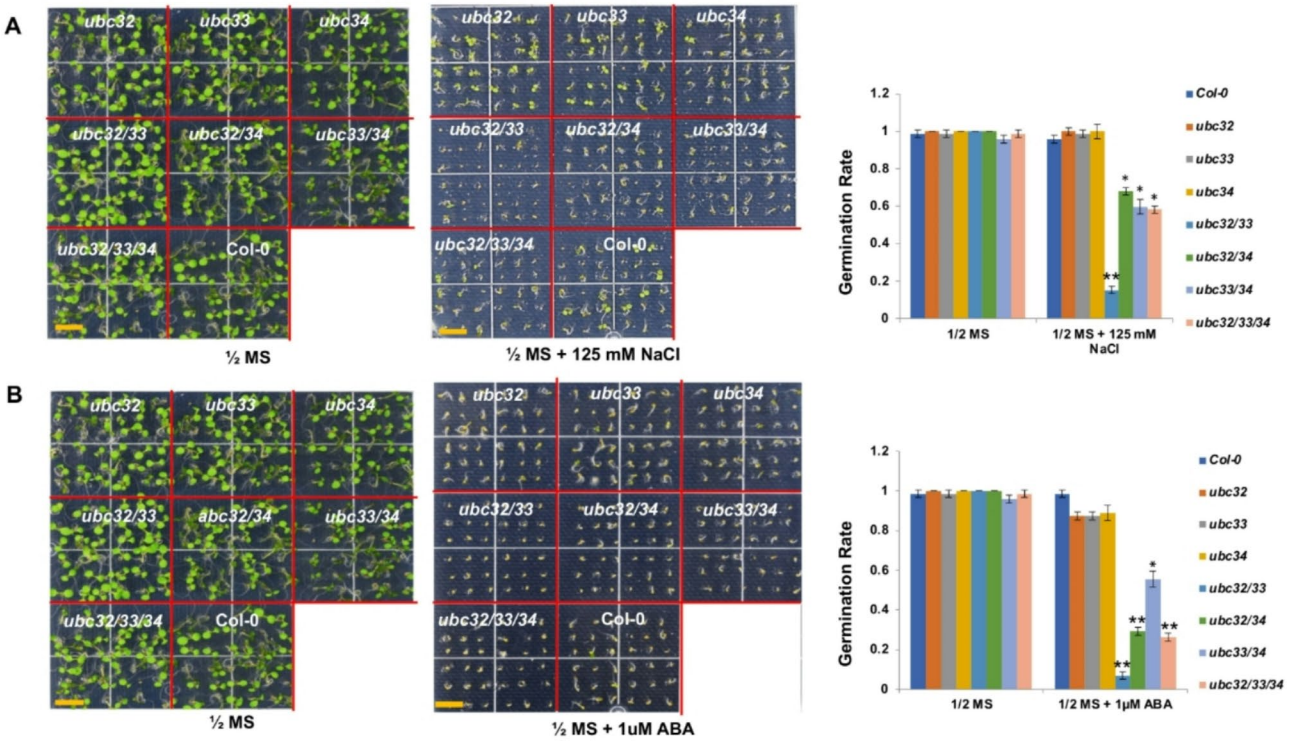

Fig. 6 *Arabidopsis* UBC32, UBC33, and UBC34 play differential roles in Salt- and ABA-induced suppression of seed germination. (**A**) The phenotypes of *Arabidopsis ubc32*, *ubc33* and *ubc34* single, double and triple mutant lines grew on half-strength Murashige and Skoog medium (½ MS) media and ½ MS media with 125mM NaCl in seed germination assay (yellow bar = 1.0 cm) (left panel). Col-0 was used as control. The percentages of different phenotypes are shown in the right panel. (**B**) The phenotypes of different Arabidopsis *ubc32*, *ubc33* and *ubc34* mutant lines grew on ½ MS media and ½ MS media with 1 μM ABA in seed germination assay (yellow bar = 1.0 cm) (left panel). Col-0 was used as control. The percentages of different phenotypes are shown in the right panels. Representative images of three independent experiments are shown. The same image of Col-0 and different Arabidopsis *ubc32*, *ubc33* and *ubc34* mutant lines grown on the ½ MS media was used in (**A**) and (**B**) as control. Photos were taken 4 days after sowing cold stratification-processed seeds on the growth media. Statistical analysis was performed using Student's t-test. *, $p \le 0.05$. **, $p \le 0.01$

or *AtUBC34* in the *atubc32* background suppressed the elevated ER-stress tolerance caused by the *atubc32* mutation. Nevertheless, the *atubc33*/*34* double mutant did not show a synergistic effect of *atubc33* and *atubc34* in reducing ER stress tolerance. Similarly, stable *N. benthamiana* transgenic *NbUBC32i* lines displayed elevated ER-stress tolerance, whereas *NbUBC33/34* RNA*i* lines showed reduced ER-stress tolerance (Supplementary Fig. 8B). Interestingly, the expression of the *UBC32* gene is significantly induced upon TM treatment in plants where *UBC33* and/or *UBC34* are knocked out or knocked down. In contrast, the expression of *UBC33* and *UBC34* does not show significant changes in plants where UBC32 is knocked out or knocked down (Supplementary Fig. 9). These findings suggest that UBC32 acts as a negative regulator, whereas UBC33 and UBC34 function as positive regulators in TM-induced ER stress tolerance. Furthermore, the results indicate the presence of a feedback in the regulation of TM-induced ER stress tolerance among these three E2 genes: *UBC32* expression is significantly upregulated when *UBC33* and/or *UBC34* are disrupted, though the reverse does not occur.

AtUBC32, AtUBC33 and AtUBC34 are involved in abiotic stress responses

Previous studies have shown that the AtUBC32 is essential for salt and drought stress responses [27, 28]. The confirmation of AtUBC33 and AtUBC34 as active components of the ERAD apparatus and their involvement in plant immunity prompted us to test if they also play key roles in plant abiotic stress responses. To this end, we examined the roles for AtUBC32, AtUBC33 and AtUBC34 in plant response to salt and abscisic acid (ABA) treatment by monitoring the seed germination rates of the single, double and triple mutants of *AtUBC32*, *AtUBC33* and *AtUBC34*. As shown in Fig. 6A, all the tested lines germinated normally on half-strength Murashige and Skoog (MS) medium, with no noticeable difference in seed germination rates. However, when exposed to 125 mM NaCl, the germination rate for all lines significantly decreased, and the extent of this reduction varied among the lines. The three single mutant lines, *atubc32*, *atubc33*, and *atubc34* exhibited germination rate comparable to Col-0 on the half-strength MS medium with 125 mM NaCl. In contrast, the three

double mutants, *atubc32/33*, *atubc32/34*, and *atubc33/34* showed significantly greater reduction in germination rate compared to Col-0. Interestingly, these double mutants displayed distinct sensitivities to salt stress, with *atubc32/33* being more sensitive than *atubc32/34*, and *atubc33/34*. The triple mutant *atubc32/33/34* showed a germination rate comparable to that of *atubc32/34*, and *atubc33/34*. These results suggest that, although AtUBC32, AtUBC33, and AtUBC34 are phylogenetically classified into the same subgroup, their roles differ in salt stress response. Synergistic effects apparently exist between AtUBC32 and AtUBC33, AtUBC33 and AtUBC34, as well as AtUBC32 and AtUBC34 in their role in seed germination under salt stress.

Similarly, adding 1 μM ABA to the half-strength MS medium significantly suppressed the germination rate of all tested lines, with variations observed among the lines (Fig. 6B). The mutant lines exhibited a response pattern similar to that observed under salt treatment: the three single mutant lines *atubc32*, *atubc33*, and *atubc34* had germination rate comparable to Col-0 under the ABA treatment, whereas the three double mutants, *atubc32/33*, *atubc32/34*, and *atubc33/34* showed a significantly greater reduction in germination rate comparted to Col-0, with different sensitivity to ABA treatment among them. The *atubc32/33/34* triple mutant displayed a reduction in seed germination comparable to the *ubc33/34* double mutant. The results suggested that, like salt stress response, synergistic effects exist between AtUBC32 and AtUBC33, AtUBC33 and AtUBC34, as well as AtUBC32 and AtUBC34 in their role in seed germination under ABA treatment.

Discussion

The importance of ERAD in plant stress tolerance and development has gained increasing recognition in recent years. However, our understanding of the components of the plant ERAD apparatus, particularly the ubiquitin-conjugating enzymes (E2s), remains limited. This knowledge gap underscores the need for further investigation into this group of enzymes, especially since several plant E2s have been shown to play active roles in plant growth, development, and responses to environmental stimuli [37]. Additionally, E2 enzymes significantly influence the length and topology of polyubiquitin chain formation as well as the processivity of ubiquitin chain elongation during ubiquitination [38]. In this study, we demonstrate that members of a ubiquitin E2 triplet—UBC32, UBC33, and UBC34 from tomato and Arabidopsis—are involved in ERAD and function in host immunity against bacterial pathogens. This suggests that the roles of this E2 triplet in ERAD and host immunity may be conserved across different plant species. Furthermore, we found that AtUBC32, AtUBC33, and AtUBC34 also contribute to plant tolerance to ER stress induced by the glycosylation inhibitor Tunicamycin (TM) and to abiotic stress. Genome-wide transcriptome analyses of ubiquitin E2 genes in potato (*Solanum tuberosum*), wheat (*Triticum aestivum L.*), and grape (*Vitis vinifera*), along with other studies, suggest that various E2 genes are involved in plant growth, development, and abiotic stress tolerance [37, 39–41]. Recently, Group III E2 enzymes from tomato were shown to contribute to plant biotic stress tolerance and are exploited by the bacterial effector AvrPtoB to suppress plant immunity [26]. However, very few E2 enzymes have been demonstrated to be involved in both ERAD and stress tolerance, both abiotic and biotic. In contrast to yeast, where Ubc6 is the only ER-localized E2 involved in ERAD [42], our findings suggest that at least three plant E2s are implicated in ERAD and play important roles in both abiotic and biotic stress tolerance. This raises the questions of how these E2s function in relation to each other and whether involvement of these E2s in ERAD directly contributes to their roles in abiotic and biotic stress tolerance. Identifying and characterizing mutants of these E2s that block their ER-localization but do not impair their E2 enzyme activities in future experiments would help address the latter question.

Using single, double and triple mutants of the Arabidopsis *UBC32*, *UBC33*, and *UBC34* genes, we revealed that members of the E2 triplet function differentially in plant tolerance to abiotic stress and TM-induced ER stress. While mutation of *AtUBC32* promotes plant tolerance to TM-induced ER stress, loss of function in *AtUBC33* or *AtUBC34* suppresses this tolerance. Interestingly, transgenic *N. benthamiana* plants in which the expression of *UBC32* or *UBC33/34* is knocked down displayed similar effects on TM-induced ER stress, suggesting the functions of these E2 Enzymes in TM-induced ER stress tolerance might also be conserved across different plant species. Unlike TM-induced ER stress, however, the *atubc32/33* double mutant displayed significantly reduced tolerance to salt- and ABA-induced suppression of seed germination, whereas the *atubc34* null mutation antagonized this effect.

Our findings indicate that, in addition to their roles in abiotic stress tolerance, UBC32, UBC33 and UBC34 also function in biotic stress. Notably, although the bacterial growth in Arabidopsis *UBC32* knockout mutant (*atubc32*) and *N. benthamiana NbUBC32i* knockdown plants was significant higher compared to control plants, the increase was always lower than that in the Arabidopsis *atubc33/34* mutant plants and *N. benthamiana NbUBC33/34i* plants (Fig. 4E, F, and G). This suggests that UBC33 and UBC34 together contribute more to plant immunity than UBC32. The diminished plant immunity in the *ubc33/ubc34* mutant plants aligns with the reduced ER stress tolerance observed, as ER

stress tolerance has been shown to be required for plant immunity [33, 35]. In contrast, the *atubc32* mutant displays diminished immunity yet elevated TM-induced ER stress tolerance, which suggests ER stress tolerance is not the sole factor that contributes to UBC32's role in host immunity, and that UBC32 may modulate multiple pathways. Indeed, previous reports indicated that UBC32, as an ERAD component, negatively regulate ER stress tolerance and salt tolerance but positively regulate oxidative burst tolerance [23, 27]. It is likely that the UBC32, UBC33 and UBC34 function in ERAD to target substrates of different pathways, and the combined actions of these E2s determine the outcome of the three E2s-mediated ERAD in modulating plant immunity. In this regard, identifying and characterizing key substrates of the E2 triplet-mediated ERAD associated with plant immunity would deepen our understanding of the role of ERAD in regulating host immunity.

The observation that the *atubc32* mutant displays increased plant tolerance to TM-induced ER is consistent with a previous report [27]. However, we did not observe a noticeable change in salt-induced suppression of seed gemination in single mutants (*atubc32*, *atubc33*, and *atubc34*) compared to Col-0. In contrast, the same previous study found that mutation of *AtUBC32* increases plant tolerance to salt stress, as evidenced by better growth of the mutant seedlings than Col-0 under 125 mM NaCl treatment [27]. This discrepancy is likely due to the different durations of salt treatment and the different readouts used to measure the plant stress responses. Seed germination is modulated by a highly complex network of signaling that includes multiple key regulators, especially the hormone abscisic acid (ABA) [42]. Salt treatment induces osmotic stress and ionic stress by reducing the seed's ability to absorb water and causing an ion imbalance within the seed, respectively. These stresses ultimately inhibit seed germination. Additionally, salt treatment induces reactive oxygen species (ROS) production and Ca^{2+} release from ER to stimulate unfolded protein response (UPR) [30]. Interestingly, the *atubc32* mutant was previously shown to exhibit less sensitivity to ion toxicity but increased sensitivity to oxidative stress [23, 27]. Thus, the impact of *atubc32* mutation on salt stress-induced suppression of seed germination is a combination of these different effects. Unlike the single mutants, we observed significantly enhanced suppression of seed germination in double and triple mutants of the three E2 genes, especially for the *atubc32/33* double mutant, confirming a role for these E2s in abiotic stress tolerance.

Our results suggest the functional relationship among members of the UBC32/33/34 E2 triplet are highly complex, depending on the type of stress involved and the specific members being examined. In addition to the antagonistic effect of UBC32 against UBC33/34 in TM-induced ER stress tolerance, synergistic effects were also observed among the members of the E2 triplet. For instance, synergistic effects apparently exist between AtUBC32 and AtUBC33, AtUBC33 and AtUBC34, as well as AtUBC32 and AtUBC34 in their roles in seed germination under salt stress and ABA treatment. Moreover, a feedback effect at the transcriptional level exists between *UBC32* and *UBC33*/*UBC34* in TM-induced ER stress tolerance. In mutant lines where the *UBC33* and/or *UBC34* gene is mutated (*atubc33*, *atubc34* and *atubc33/34*), the expression of the *UBC32* gene was significantly induced under TM-induced ER stress (Supplementary Fig. 9). A similar effect was also observed in *NbUBC33/34i* lines where the two genes are knocked down. Interestingly, the expression of the *UBC33* and *UBC34* gene was not significantly altered in the *ubc32* mutant under TM-induced ER stress. Additionally, a feedback loop likely exists in the cell, where the synergistic effects of *AtUBC32*, *AtUBC33*, and *AtUBC34* in seed germination under salt stress and ABA treatment, as well as in host immunity, are partially compensated—likely by another ER-associated E2 (or E2s)—when *AtUBC32*, *AtUBC33*, and *AtUBC34* are all mutated. In addition to UBE2J1/UBE2J2, which are homologs of the Arabidopsis AtUBC32/AtUBC33/AtUBC34 (Supplementary Fig. 10), animal E2 enzymes UBE2G2/UBC7 have also been implicated in ERAD [20]. The Arabidopsis E2 enzymes AtUBC7 (At5g05460), AtUBC13 (At3g46460), and AtUBC14 (At3g46470) are close homologs of UBE2G2/UBC7 in phylogenetic analysis (Supplementary Fig. 10 and Supplementary Data File II) and have been implicated in multiple abiotic stresses tolerance [43]. Future experiments could determine whether these E2s compensate for ERAD function when *AtUBC32*, *AtUBC33*, and *AtUBC34* are all mutated.

While ERAD is critically important under stress conditions, its activity must be maintained at a low level under steady-state conditions where fewer misfolded proteins accumulate. Reduction of ERAD activity can be achieved by degradation of ERAD components and/or disassembly of the ERAD complex, with the former referred to as ERAD tuning [44]. Indeed, Arabidopsis UBC32 was previously shown to work with DOA10 for ERAD while itself being a substrate of the HRD1 pathway-dependent ERAD [22]. However, the E2 enzyme working with HRD1 in the ubiquitination/targeting of UBC32 was not identified [22]. This study indicates that the *atubc33* and *atubc34* mutations counteract the enhanced plant tolerance to TM-induced ER stress mediated by the *atubc32* mutant. Furthermore, UBC33 and UBC34 interact strongly with the HRD1 homologs in tomato. Combining these findings, it is reasonable to speculate that UBC33 and/or UBC34 may be employed by HRD1 in targeting UBC32 for ERAD tuning. Future experiments

addressing this hypothesis would further elucidate the relationship between members of the E2 triplet in ERAD and the dynamics of ERAD under different physiological conditions.

To date, many components of the ERAD apparatus, as well as mechanisms for modulating the ERAD activity are found to be conserved between plants and animals. The HRD1-mediated degradation of UBC32 and its homolog UBE2J1, for instance, has been shown to be conserved in plants and mammals. Previously, our phylogenetic analysis showed that UBC32 and mammalian E2 UBE2J1 are classified into the same sub-clade, whereas UBC33/34 and mammalian E2 UBE2J2 are closely related [45]. UBE2J1 was shown to be a substrate of the mitogen-activated protein kinase (MAPK) p38 under stress condition [46]. Given the conservation of ERAD between plants and mammals, it would be intriguing to investigate whether UBC32, UBC33, and/or UBC34 are also modified by posttranslational modifications for modulating its activity in ERAD. While such modifications of E2 enzymes have not been identified in plants, they have been well characterized in humans, animals and yeast [3].

Conclusion

This study establishes that the ubiquitin E2 enzymes UBC32, UBC33, and UBC34 in tomato (*Solanum lycopersicum*) and *Arabidopsis thaliana* are involved in ER-associated protein degradation (ERAD) and play pivotal roles in plant tolerance to abiotic stresses, as well as host immunity against bacterial pathogens. We further demonstrate that AtUBC32, AtUBC33, and AtUBC34 contribute significantly to plant tolerance to ER stress induced by the glycosylation inhibitor tunicamycin (TM). These findings, combined with previous reports [21, 24, 27], suggest that, unlike in yeast, multiple ubiquitin E2 enzymes participate in plant ERAD. Despite belonging to the same clade in the phylogenetic tree of ubiquitin E2 enzymes, UBC32, UBC33, and UBC34 exhibit redundant, synergistic, or antagonistic roles depending on the specific stress tolerance pathway examined, underscoring the complexity of their functional interactions.

Methods

Growth of Bacteria and plant materials

Agrobacterium tumefaciens (strain GV3101) and *Pseudomonas syringae* pv *tomato (Pst)* were grown at 28 °C on Luria-Bertani and King's B medium, respectively with appropriate antibiotics. Tobacco (*Nicotiana benthamiana*) and tomato RG-pto11 (*pto11/pto11*, *Prf/Prf*) seeds were germinated, and plants were grown on autoclaved soil in a growth chamber with 16 h light (~300 µmol/m^2/s at the leaf surface of the plants), 24°C/23°C day/night temperature, and 50% relative humidity.

Transgenic *N. benthamiana* lines (*NbUBC32i* and *NbUBC33/34i*), in which *NbUBC32* or *NbUBC33/UBC34* genes were knocked down, were generated via standard *Agrobacterium*-mediated transformation [47]. Briefly, a 200-bp fragment common to *NbUBC32* genes and a 330-bp fragment common to *NbUBC33* and *NbUBC34* genes were amplified from *N. benthamiana* cDNA using the primer pairs NbUBC32-RNAi-XhoI-PstI-F and NbUBC32-RNAi-HindIII-EcoRI-R, and NbUBC33/34-RNAi-XhoI-PstI-F and NbUBC33/34-RNAi-HindIII-EcoRI-R, respectively. The purified PCR products were digested with restriction enzymes as indicated in the primer names and cloned into the Gateway-compatible vector pBTEX-GW to generate RNA interference (RNAi) constructs. Following sequence verification, these RNAi constructs were introduced into the *Agrobacterium* strain EHA105 for transformation.

Arabidopsis mutant lines SALK_082711 (*atubc32*) [27], SALK_104882C (*atubc33*) and CS878883 (*atubc34*) [28] were obtained from Arabidopsis Biological Resource Center (ABRC). Arabidopsis plants were grown in a growth chamber with 16 h light (~300 µmol/m^2/s at the leaf surface of the plants), 22°C/22°C day/night temperature, and 50% relative humidity.

DNA manipulations and plasmid constructions

Standard molecular biology techniques were used for all DNA manipulations [48]. Open reading frames (ORFs) of genes of interest were amplified using Q5 high-fidelity DNA polymerase (New England Biolabs). All constructs used in this study were sequence-verified. The *MLO-12* mutant of the barley *MLO* gene was generated by amplifying two overlapping fragments of the ORF using the primer pairs MLO-GW-F/MLO(F240L)-R, and MLO(F240L)-F/MLO-GW-R, which flank the mutation site (F240L) (Supplementary Table I) [32]. These fragments were amplified from cDNA synthesized using total RNA extracted from barley (*Hordeum vulgare* cv. Golden Promise) seedlings. The overlapping PCR products were combined as a template for amplifying the full *MLO-12* ORF containing the F240L mutation by primer pairs MLO-GW-F/MLO-GW-R. All cloned genes and virus-induced gene silencing (VIGS) fragments were inserted into the pENTR/SD/D-TOPO entry vector using Gateway cloning (Invitrogen), followed by cloning into the corresponding expression vectors. Expression vectors used in this study included pDEST15 (GST-tagged protein expression), pDEST17 (6HIS-tagged protein expression), and the mating-based split-ubiquitin system (ordered from ABRC; MetYC_GW for CubPLV-fused bait proteins and NX32_GW for NubG-fused prey proteins). For plant expression, constructs included PLN462-MLO-12 (HA-tagged MLO-12) [49], pGWB5 and pGWB6 (GFP-fused protein localization) [50], and

BiFC vectors pSCYNE/pSCYCE (for protoplast assays) and pSPYCE(M)/pSPYNE(R)173 (for tobacco leaf assays) [51]. The TRV2 vector was used for VIGS. The TRV-*SlUBC32/33/34* construct used for silencing the tomato *UBC32*, *UBC33*, and *UBC34* genes together was cloned using a previously described strategy [26]. Briefly, DNA fragments targeting *SlUBC32*, *SlUBC33*, and *SlUBC34*, respectively were first amplified using plasmid DNA of corresponding gene as template by overlapping primer pairs SlUbc32VIGS-F/SlUbc32VIGS-R, SlUbc33VIGS-F/SlUbc33VIGS-R, SlUbc34VIGS-F/SlUbc34VIGS-R. The PCR products were combined as a template for amplifying the insert by the primer pairs SlUbc32VIGS-F/SlUbc34VIGS-R, followed by cloning into the vector TRV2. Primers used for this study are listed in Supplementary Table I.

Sequence alignment and phylogenetic analysis

Protein sequences were aligned using ClustalX 2.1 [52]. The phylogenetic analysis was then performed with the MEGA software using the aligned sequences [53]. To build an unrooted phylogenetic tree, the evolutionary history was inferred using the neighbor-joining method with 500 bootstrap trials, and evolutionary distances were calculated using the p-distance method [54]. Branches with bootstrap support < 50% were collapsed in the tree.

Expression and purification of Recombinant proteins

Recombinant proteins were expressed in *Escherichia coli* strain BL21 (DE3) and purified with standard protocol [48]. Purified proteins were desalted and concentrated in storage buffer (50 mM Tris-HCl pH 8.0, 50 mM KCl, 0.1 mM EDTA, 1 mM DTT, 0.5 mM PMSF) using Amicon centrifugal filters (Millipore). The final protein concentration was determined using the Bio-Rad protein assay reagent, and proteins were stored at -80 °C in 40% glycerol.

Yeast Two-Hybrid

The interactions of SlHRD1A, SlHRD1B and SlHRD3A with SlUBC32, SlUBC33 and SlUBC34 were detected using the mating-based split-ubiquitin system (mbSUS) [31]. Bait vectors carrying Cub-fused sequences and prey vectors carrying Nub-fused sequences were transformed into yeast strains THY.AP4 and THY.AP5, respectively, using polyethylene glycol (PEG)-mediated transformation. SC- minimal media (synthetic complete minimal media plus amino acids dropout mix) with ADE, HIS, TRP and URA, and SC-minimal media with ADE, HIS and LEU were used for selection of positive THY.AP4 and THY.AP5 transformants, respectively. Yeast mating was performed on YPD media at 28 °C for four days. The mating cells were then transferred using toothpicks to a 96-well plate with 100 µL of sterilized ddH_2O in each well, and 8 µL of each mating cells were dropped onto SC-minimal media plates and SC-ADE + HIS + media plates, respectively. The SC-ADE + HIS + media served as the growth control. After 3–7 days, Positive interactions were determined based on cell growth, and methionine concentrations were adjusted to optimize signal-to-noise ratio.

Quantitative real time-PCR (qRT-PCR)

Gene expression was analyzed in *N. benthamiana* E2-RNAi lines, VIGS-treated plants, and Arabidopsis plants subjected to different treatments. Leaf tissues of 3- to 4-week-old plants were collected for total RNA extraction using the RNeasy Plant Mini Kit with DNase treatment (QIAGEN) by following the protocol provided by the manufacturer. cDNA was synthesized using Superscript III reverse transcriptase and oligo(dT) primers (Life Technologies). qRT-PCR was performed using SYBR Green (Life Technologies) on a LightCycler 480 (Roche) or iCycler (Bio-Rad). All primers used in qRT-PCR are showed in the Supplementary Table I. Standard comparative C_t method was used for calculating the relative expression level of tested genes, with the relative expression level of the internal reference gene at untreated or 0 h after treatment set as 1 [55]. *SlEF1a*, *NbEF1a* and *AtActin2* were used as the internal references for tomato, *N. benthamiana* and Arabidopsis samples, respectively. All qRT-PCR experiments were performed with three technical repeats in each of the three biological replicates.

Bimolecular fluorescence complementation (BiFC) assay

The BiFC assay that is based on split yellow fluorescent protein (YFP) was used to test the protein interaction in protoplasts derived from tomato leaves and on tobacco leaves [51, 56]. The empty vectors (nYFP-EV and cYFP-EV) were used as negative controls. Protoplasts were prepared as described [57], And approximately 1×10^4 protoplasts were co-transfected with 10 µg of plasmid DNA of each construct. The co-transfected protoplast was imaged 21 h after transfection using an Olympus FV500 Inverted (Olympus IX-81) confocal microscope with the following excitation and emission wavelengths: YFP, 514.5 nm (excitation) and 525 to 555 nm (emission); chlorophyll autofluorescence, 640.5 nm (excitation) and 663 to 738 nm (emission). For BiFC assays on *N. benthamiana* leaves, the pSPYNE173 and pSPYCE(M) constructs expressing different proteins of interest were co-introduced into 4-week-old tobacco leaves by Agro-inflitration. Fluorescence signals were detected by confocal microscopy 48 h after Agro-infiltration.

Virus-Induced gene Silencing (VIGS)

Gene silencing was induced using the tobacco rattle virus (TRV) vectors as previously described [58, 59]. *Agrobacterium* (OD_{600} = 0.5) containing appropriate pTRV plasmids was induced with acetosyringone and used to infiltrate two leaf-stage tomato seedlings and 3-week-old tobacco seedlings. VIGS-treated plants were maintained under 16 h light/8 h night, 21°C/21°C (tomato) or 24°C/22°C (tobacco) conditions for 3–4 weeks to allow silencing to take effect.

Plant protein extraction and Immuno-blotting

Each Arabidopsis sample was homogenized in 300 µL protein extraction buffer (25 mM Tris-HCl, pH 7.5, 150 mM NaCl, 5% glycerol, 0.05% Nonidet P-40, 2.5 mM EDTA, 1 mM phenylmethylsulfonyl fluoride and 1× complete cocktail of protease inhibitors). The concentration of total proteins was determined using protein assay agent (Bio-Rad). Each sample containing 20 µg of proteins was added with 2× SDS protein loading buffer, boiled for 5 min, and then resolved by 10% SDS-PAGE. Immunoblotting was performed with appropriate antibodies: anti-FLAG (Sigma) and anti-HA (Sigma).

Bacterial population assay

The bacterial population assay was conducted as described [60, 61]. Briefly, for assaying the growth of *Pst* strains DC3000 and DC3000*ΔhrcQ-U*, Arabidopsis or tomato plants about four weeks after VIGS infection were inoculated with the suspension of pathogen DC3000 (1×10^6 CFU/mL) and DC3000*ΔhrcQ-U* (1×10^9 CFU/mL) containing 0.002% Silwet L-77 and 10 mM $MgCl_2$ by vacuum infiltration. Additionally, the dipping method was also used to inoculate tomato plants with DC3000*ΔhrcQ-U* (1×10^9 CFU/mL). Inoculated plants were maintained in a growth chamber and monitored daily for symptom development. To assess bacterial populations, leaf discs were harvested from three to four plants of each treatment on day 3 and day 4 after the inoculation, ground, serially diluted, and plated to determine the amount of the bacteria grown as described.

Experiments in Figs. 1, 2A and B and 4A, and 4B were repeated with two biological replicates. All other experiments were conducted with three biological replicates.

Supplementary Information

The online version contains supplementary material available at https://doi.org/10.1186/s12870-025-06419-8.

Supplementary Material 1

Supplementary Material 2: **Fig. 1**. Protein sequence alignment of tomato SlUBC32, SlUBC33, and SlUBC34 with their Arabidopsis and human homologs. **Fig. 2**. Protein sequence alignment of tomato HRD1A and HRD1B with their Arabidopsis and human homologs. **Fig. 3**. SlHARD1A and SlHARD1B interact with members of the SlUBC32, SlUBC33, and SlUBC34 triplet at ER. **Fig. 4**. Identification of single, double and triple mutants of the Arabidopsis AtUBC32, AtUBC33, and AtUBC34 genes. **Fig. 5**. Morphology of single, double and triple mutants of the Arabidopsis AtUBC32, AtUBC33, and AtUBC34 genes. **Fig. 6**. Morphology and flowering time of single, double and triple mutants of the Arabidopsis AtUBC32, AtUBC33, and AtUBC34 genes. **Fig. 7**. UBC32, UBC33 and UBC34 are involved in plant immunity. **Fig. 8**. UBC32, UBC33 and UBC34 are involved in plant ER stress response. **Fig. 9**. The transcript level of the UBC32, UBC33 and UBC34 genes in Arabidopsis different mutant lines and N. benthamiana RNAi transgenic lines. **Fig. 10**. Phylogeny of the human and Arabidopsis E2 enzymes and E2 variants.

Supplementary Material 3: **Table I**. List of primers used in this study.

Supplementary Material 4: **Data file I**. Tomato HRD1A, HRD1B, HRD3A CDS and protein sequences.

Supplementary Material 5: **Data file II**. Amino acid sequences of Arabidopsis and human ubiquitin E2 enzymes and E2 variants.

Acknowledgements

We thank Christian Elowsky and You Zhou (Biotechnology Center, University of Nebraska-Lincoln) for helping with the confocal microscope. We are grateful to Harkamal Walia for sharing the barley seeds for cloning the MLO gene. We also thank the Arabidopsis Biological Resource Center for the Arabidopsis T-DNA insertion lines.

Author contributions

C.W. examined the accumulation of MLO-12 in tobacco UBC32i and UBC33/34i transgenic lines, confirmed the Arabidopsis ubc32/33/34 triple mutant and morphology of the single, double and triple mutants of Arabidopsis AtUBC32, AtUBC33, and AtUBC34 genes, examined the subcellular localization of tomato SlUBC32, SlUBC33, SlUBC34, SlHRD1A and SlHRD1B, wrote and edited the manuscript. B.Z. designed experiments, identified the Arabidopsis ubc32, ubc33, and ubc34 single, double and triple mutants, performed most experiments, and analyzed data. Y. Z. examined the subcellular localization of tomato SlHRD1A and SlHRD1B. L.Z. designed experiments, analyzed the data, wrote and edited the manuscript.

Funding

This work was supported by start-up funds from the University of Nebraska-Lincoln, the U.S. Department of Agriculture National Institute of Food and Agriculture (grant no. 2012-67014-19449), and the National Science Foundation (grant no. IOS-1645659) to L.Z.

Data availability

The datasets generated and/or analyzed during the current study are available in the GenBank library of National Center for Biotechnology Information (NCBI), https://www.ncbi.nlm.nih.gov/genbank/ and the Nicotiana benthamiana and tabacum Omics database, http://lifenglab.hzau.edu.cn/Nicomics/index.php [62]. Sequence data of tomato and Arabidopsis genes that were used in this article can be found in the GenBank library with the following accession numbers: ***SlUBC32*** (KY246924); ***SlUBC33*** (KY246925); ***SlUBC34*** (KY246926); ***SlHRD1A*** (XM_026030007); ***SlHRD1B*** (XM_004241394); ***SlHRD3A*** (XM_004235721); ***AtHRD1A*** (NM_112479); ***AtHRD1B*** (NM_179512); ***AtHRD3a*** (NM_101684); ***AtUBC32*** / ***AT3G17000*** (NM_112576); ***AtUBC33*** / ***AT5G50430*** (NM_124425); ***AtUBC34*** / ***AT1G17280*** (NM_001084085). Sequence data of corresponding ***N. benthamiana*** E2 genes can be found at the Nicotiana benthamiana and tabacum Omics database, http://lifenglab.hzau.edu.cn/Nicomics/index.php with the following accession numbers ***NbUBC32a*** (Nbe17g29580.1) and ***NbUBC32b*** (Nbe18g03100.1), ***NbUBC33a*** (Nbe05g34910.1) and ***NbUBC33b*** (Nbe06g26060.1), ***NbUBC34a*** (Nbe10g19520.1) and ***NbUBC34b*** (Nbe05g02070.1).

Declarations

Ethics approval and consent to participate

Not applicable.

Consent for publication

Not applicable.

Competing interests
The authors declare no competing interests.

Clinical trial number
Not applicable.

Received: 22 January 2025 / Accepted: 18 March 2025
Published online: 02 April 2025

References

1. Zhang H, Zhu J, Gong Z, Zhu J. Abiotic stress responses in plants. Nat Rev Genet. 2022;23(2):104–19.
2. Ngou BPM, Ding P, Jones JDG. Thirty years of resistance: Zig-zag through the plant immune system. Plant Cell. 2022;34(5):1447–78.
3. Zhang Y, Zeng L. Crosstalk between ubiquitination and other Post-translational protein modifications in plant immunity. Plant Commun 2020:100041.
4. Miricescu A, Goslin K, Graciet E. Ubiquitylation in plants: signaling hub for the integration of environmental signals. J Exp Bot. 2018;69(19):4511–27.
5. Xu F, Xue H. The ubiquitin-proteasome system in plant responses to environments. Plant Cell Environ. 2019;42(10):2931–44.
6. Su Y, Ngea G, Wang K, Lu Y, Godana E, Ackah M, Yang Q, Zhang H. Deciphering the mechanism of E3 ubiquitin ligases in plant responses to abiotic and biotic stresses and perspectives on protacs for crop resistance. Plant Biotechnol J. 2024;22(10):2811–43.
7. Zhu J. Abiotic stress signaling and responses in plants. Cell. 2016;167(2):313–24.
8. Ma X, Claus LAN, Leslie ME, Tao K, Wu Z, Liu J, Yu X, Li B, Zhou J, Savatin DV, et al. Ligand-induced monoubiquitination of BIK1 regulates plant immunity. Nature. 2020;581(7807):199–203.
9. Saeed B, Deligne F, Brillada C, Dünser K, Ditengou F, Turek I, Allahham A, Grujic N, Dagdas Y, Ott T, et al. K63-linked ubiquitin chains are a global signal for endocytosis and contribute to selective autophagy in plants. Curr Biol. 2023;33(7):1337–e455.
10. Smalle J, Vierstra RD. The ubiquitin 26S proteasome proteolytic pathway. Annu Rev Plant Biol. 2004;55:555–90.
11. Ye Y, Rape M. Building ubiquitin chains: E2 enzymes at work. Nat Rev Mol Cell Biol. 2009;10(11):755–64.
12. Li C, Xia B, Wang S, Xu J. Folded or Degraded in Endoplasmic Reticulum. In: *Regulation of Cancer Immune Checkpoints.* Edited by Jie Xu. Singapore: Springer; 2020: 265– 94.
13. Buchberger A, Bukau B, Sommer T. Protein quality control in the cytosol and the Endoplasmic reticulum: brothers in arms. Mol Cell. 2010;40(2):238–52.
14. Strasser R. Protein quality control in the Endoplasmic reticulum of plants. Annu Rev Plant Biol. 2018;69:147–72.
15. Yoshida H. ER stress and diseases. FEBS J. 2007;274(3):630–58.
16. Guerriero C, Brodsky J. The delicate balance between secreted protein folding and Endoplasmic reticulum-associated degradation in human physiology. Physiol Rev. 2012;92(2):537–76.
17. Chen Q, Yu F, Xie Q. Insights into Endoplasmic reticulum-associated degradation in plants. New Phytol. 2020;226(2):345–50.
18. Wang X, Herr R, Rabelink M, Hoeben R, Wiertz E, Hansen T. Ube2j2 ubiquitinates hydroxylated amino acids on ER-associated degradation substrates. J Cell Biol. 2009;187(5):655–68.
19. Burr M, Cano F, Svobodova S, Boyle L, Boname J, Lehner P. HRD1 and UBE2J1 target misfolded MHC class I heavy chains for Endoplasmic reticulum-associated degradation. Proc Natl Acad Sci U S A. 2011;108(5):2034–9.
20. Chen B, Mariano J, Tsai Y, Chan A, Cohen M, Weissman A. The activity of a human Endoplasmic reticulum-associated degradation E3, gp78, requires its cue domain, RING finger, and an E2-binding site. Proc Natl Acad Sci U S A. 2006;103(2):341–6.
21. Li J, Zhang B, Duan P, Yan L, Yu H, Zhang L, Li N, Zheng L, Chai T, Xu R, et al. An Endoplasmic reticulum-associated degradation-related E2-E3 enzyme pair controls grain size and weight through the brassinosteroid signaling pathway in rice. Plant Cell. 2023;35(3):1076–91.
22. Chen Q, Zhong Y, Wu Y, Liu L, Wang P, Liu R, Cui F, Li Q, Yang X, Fang S et al. HRD1-mediated ERAD tuning of ER-bound E2 is conserved between plants and mammals. In: *Nat Plants.* vol. 2; 2016: 16094.
23. Cui F, Liu L, Li Q, Yang C, Xie Q. UBC32 mediated oxidative tolerance in Arabidopsis. J Genet Genomics. 2012;39(8):415–7.
24. Wang Y, Yue J, Yang N, Zheng C, Zheng Y, Wu X, Yang J, Zhang H, Liu L, Ning Y, et al. An ERAD-related ubiquitin-conjugating enzyme boosts broad-spectrum disease resistance and yield in rice. Nat Food. 2023;4(9):774–87.
25. Kraft E, Stone SL, Ma L, Su N, Gao Y, Lau O-S, Deng X-W, Callis J. Genome analysis and functional characterization of the E2 and RING-type E3 ligase ubiquitination enzymes of Arabidopsis. Plant Physiol. 2005;139(4):1597–611.
26. Zhou B, Mural RV, Chen X, Oates ME, Connor RA, Martin GB, Gough J, Zeng L. A subset of Ubiquitin-Conjugating enzymes is essential for plant immunity. Plant Physiol. 2017;173(2):1371–90.
27. Cui F, Liu L, Zhao Q, Zhang Z, Li Q, Lin B, Wu Y, Tang S, Xie Q. Arabidopsis ubiquitin conjugase UBC32 is an ERAD component that functions in brassinosteroid-mediated salt stress tolerance. Plant Cell. 2012;24(1):233–44.
28. Ahn M, Oh T, Seo D, Kim J, Cho N, Kim W. Arabidopsis group XIV ubiquitin-conjugating enzymes AtUBC32, AtUBC33, and AtUBC34 play negative roles in drought stress response. J Plant Physiol. 2018;230:73–9.
29. Nelson BK, Cai X, Nebenführ A. A multicolored set of in vivo organelle markers for co-localization studies in Arabidopsis and other plants. Plant J. 2007;51(6):1126–36.
30. Liu L, Cui F, Li Q, Yin B, Zhang H, Lin B, Wu Y, Xia R, Tang S, Xie Q. The Endoplasmic reticulum-associated degradation is necessary for plant salt tolerance. Cell Res. 2011;21(6):957–69.
31. Grefen C, Obrdlik P, Harter K. The determination of protein-protein interactions by the mating-based split-ubiquitin system (mbSUS). Methods Mol Biol (Clifton NJ). 2009;479:217–33.
32. Müller J, Piffanelli P, Devoto A, Miklis M, Elliott C, Ortmann B, Schulze-Lefert P, Panstruga R. Conserved ERAD-like quality control of a plant polytopic membrane protein. Plant Cell. 2005;17(1):149–63.
33. Wang D, Weaver N, Kesarwani M, Dong X. Induction of protein secretory pathway is required for systemic acquired resistance. Science. 2005;308(5724):1036–40.
34. Howell S. Endoplasmic reticulum stress responses in plants. Annu Rev Plant Biol. 2013;64:477–99.
35. Moreno A, Mukhtar M, Blanco F, Boatwright J, Moreno I, Jordan M, Chen Y, Brandizzi F, Dong X, Orellana A, et al. IRE1/bZIP60-mediated unfolded protein response plays distinct roles in plant immunity and abiotic stress responses. PLoS ONE. 2012;7(2):e31944.
36. Chakraborty R, Uddin S, Macoy DM, Park SO, Van Anh DT, Ryu GR, Kim YH, Lee J-Y, Cha J-Y, Kim W-Y, et al. Inositol-requiring enzyme 1 (IRE1) plays for AvrRpt2-triggered immunity and RIN4 cleavage in Arabidopsis under Endoplasmic reticulum (ER) stress. Plant Physiol Biochem. 2020;156:105–14.
37. Liu W, Tang X, Qi X, Fu X, Ghimire S, Ma R, Li S, Zhang N, Si H. The ubiquitin conjugating enzyme: an important ubiquitin transfer platform in ubiquitin-Proteasome system. Int J Mol Sci. 2020;21(8):2894.
38. Stewart M, Ritterhoff T, Klevit R, Brzovic P. E2 enzymes: more than just middle men. Cell Res. 2016;26(4):423–40.
39. Liu W, Tang X, Zhu X, Qi X, Zhang N, Si H. Genome-wide identification and expression analysis of the E2 gene family in potato. Mol Biol Rep. 2019;46(1):777–91.
40. Gao Y, Wang Y, Xin H, Li S, Liang Z. Involvement of Ubiquitin-Conjugating enzyme (E2 gene Family) in ripening process and response to cold and heat stress of vitis vinifera. Sci Rep. 2017;7(1):13290.
41. Gao W, Zhang L, Zhang Y, Zhang P, Shahinnia F, Chen T, Yang D. Genome–wide identification and expression analysis of the UBC gene family in wheat (*Triticum aestivum L*). BMC Plant Biol. 2024;24(1):341.
42. Sajeev N, Koornneef M, Bentsink L. A commitment for life: decades of unraveling the molecular mechanisms behind seed dormancy and germination. Plant Cell. 2024;36(5):1358–76.
43. Feng H, Wang S, Dong D, Zhou R, Wang H. Arabidopsis Ubiquitin-Conjugating enzymes UBC7, UBC13, and UBC14 are required in plant responses to multiple stress conditions. Plants (Basel) 2020, 9(6).
44. Calì T, Galli C, Olivari S, Molinari M. Segregation and rapid turnover of EDEM1 by an autophagy-like mechanism modulates standard ERAD and folding activities. Biochem Biophys Res Commun. 2008;371(3):405–10.
45. Zhou B, Zeng L. Elucidating the role of highly homologous *Nicotiana benthamiana* ubiquitin E2 gene family members in plant immunity through an improved virus-induced gene Silencing approach. Plant Methods. 2017;13(1):59.
46. Menon M, Tiedje C, Lafera J, Ronkina N, Konen T, Kotlyarov A, Gaestel M. Endoplasmic reticulum-associated ubiquitin-conjugating enzyme Ube2j1 is a novel substrate of MK2 (MAPKAP kinase-2) involved in MK2-mediated TNFα production. Biochem J. 2013;456(2):163–72.

47. Clemente T. Nicotiana (*Nicotiana tobaccum, Nicotiana benthamiana*). Methods Mol Biol. 2006;343:143–54.
48. Green MR, Sambrook J, Sambrook J. Molecular cloning: a laboratory manual. 4th ed. N.Y.: Cold Spring Harbor Laboratory Press;: Cold Spring Harbor; 2012.
49. Espinosa A, Guo M, Tam VC, Fu ZQ, Alfano JR. The *Pseudomonas syringae* type III-secreted protein HopPtoD2 possesses protein tyrosine phosphatase activity and suppresses programmed cell death in plants. Mol Microbiol. 2003;49(2):377–87.
50. Nakagawa T, Kurose T, Hino T, Tanaka K, Kawamukai M, Niwa Y, Toyooka K, Matsuoka K, Jinbo T, Kimura T. Development of series of gateway binary vectors, pGWBs, for realizing efficient construction of fusion genes for plant transformation. J Biosci Bioeng. 2007;104(1):34–41.
51. Waadt R, Schmidt LK, Lohse M, Hashimoto K, Bock R, Kudla J. Multicolor bimolecular fluorescence complementation reveals simultaneous formation of alternative CBL/CIPK complexes in planta. Plant J. 2008;56(3):505–16.
52. Larkin MA, Blackshields G, Brown NP, Chenna R, McGettigan PA, McWilliam H, Valentin F, Wallace IM, Wilm A, Lopez R, et al. Clustal W and clustal X version 2.0. Bioinformatics. 2007;23(21):2947–8.
53. Kumar S, Stecher G, Li M, Knyaz C, Tamura K. MEGA X: molecular evolutionary genetics analysis across computing platforms. Mol Biol Evol. 2018;35(6):1547–9.
54. Nei M, Kumar S. Molecular evolution and phylogenetics. Oxford; New York: Oxford University Press; 2000.
55. Schmittgen T, Livak K. Analyzing real-time PCR data by the comparative C(T) method. Nat Protoc. 2008;3(6):1101–8.
56. Chen S, Tao L, Zeng L, Vega Sanchez ME, Umemura K, Wang GL. A highly efficient transient protoplast system for analyzing defence gene expression and protein-protein interactions in rice. Mol Plant Pathol. 2006;7(5):417–27.
57. Rosebrock TR, Zeng L, Brady JJ, Abramovitch RB, Xiao F, Martin GB. A bacterial E3 ubiquitin ligase targets a host protein kinase to disrupt plant immunity. Nature. 2007;448(7151):370–4.
58. Mural RV, Liu Y, Rosebrock TR, Brady JJ, Hamera S, Connor RA, Martin GB, Zeng L. The tomato Fni3 lysine-63-specific ubiquitin-conjugating enzyme and suv ubiquitin E2 variant positively regulate plant immunity. Plant Cell. 2013;25(9):3615–31.
59. Caplan J, Dinesh-Kumar SP. Using viral vectors to silence endogenous genes. *Curr Protoc Microbiol* 2006, Chap. 16:16i.6.1-i.6.3.
60. Nguyen HP, Chakravarthy S, Velasquez AC, McLane HL, Zeng L, Nakayashiki H, Park DH, Collmer A, Martin GB. Methods to study PAMP-triggered immunity using tomato and *Nicotiana benthamiana*. Mol Plant Microbe Interact. 2010;23(8):991–9.
61. Katagiri F, Thilmony R, He SY. The Arabidopsis thaliana-*pseudomonas syringae* interaction. arabidopsis Book. 2002;1:e0039.
62. Wang J, Zhang Q, Tung J, Zhang X, Liu D, Deng Y, Tian Z, Chen H, Wang T, Yin W, et al. High-quality assembled and annotated genomes of *Nicotiana tabacum* and *Nicotiana benthamiana* reveal chromosome evolution and changes in defense arsenals. Mol Plant. 2024;17(3):423–37.

Publisher's note